Embedded ICG-based Stroke Volume Measurement System: Comparison of Discrete-Time and Continuous-Time Architectures

Antoine Gautier, Benoit Larras, Olev Märtens, Deepu John, Antoine Frappé

Embedded ICG-based Stroke Volume Measurement System: Comparison of Discrete-Time and Continuous-Time Architectures

Antoine Gautier
Univ. Lille, CNRS, Centrale Lille, Junia, Univ. Polytechnique Hauts-de-France, UMR 8520 - IEMN
Lille, France
antoine.gautier@junia.com

Benoît Larras
Univ. Lille, CNRS, Centrale Lille, Junia, Univ. Polytechnique Hauts-de-France, UMR 8520 - IEMN
Lille, France

Olev Märtens
Tallinn University of Technology, T.J. Seebeck Department of Electronics
Tallinn, Estonia

Deepu John
School of Electrical and Electronic Engineering, University College Dublin,
Republic of Ireland

Antoine Frappé
Univ. Lille, CNRS, Centrale Lille, Junia, Univ. Polytechnique Hauts-de-France, UMR 8520 - IEMN
Lille, France

***Abstract*— This paper describes the study of an integrated system for the detection of the B-C-X characteristic points of impedance cardiography (ICG) signals, to evaluate the stroke volume of a patient. It compares a discrete-time digital approach and a continuous-time digital architecture, using a level-crossing Analog-to-Digital Conversion (LC-ADC). The results show that the measurement accuracy of the stroke volume, with a relative error between 9% and 13%, is sufficient for practical use and opens the opportunity for future fully integrated circuit solutions. This study also points out that, unlike ECG, the continuous-time digital approach does not bring any improvements for ICG-based systems.**

Keywords—ICG, Stroke Volume, wearable, biosignal monitoring

I. INTRODUCTION

Impedance cardiography (ICG) is a common method for estimation and monitoring of multiple hemodynamic features including the Stroke Volume (SV) [1], [2], [3]. ICG combined with electrocardiography (ECG) shows opportunities for cost-effective cardiac monitoring [4], [5]. SV monitoring applications are numerous, and studies exhibit the interest in wearable low-power solutions for cardiac monitoring [6],[7]. The study of literature and commercial solutions show that there is no low-power and low-complexity wearable integrated circuit alternative for ICG SV monitoring, the closest implementations to wearable devices use discrete components such as Raspberry PI 3 [8] or are more portable than wearable [9] or consists in wearable ICG sensing with processing of SV done by computer [10]. The objective of this paper is to study the feasibility and accuracy of a low-complexity integrated low-power solution for SV wearable monitoring using ICG signal for further integrated circuit implementation. Two solution schemes for the detection of the ICG characteristic points and the extraction of hemodynamic features are studied in the Discrete-Time (DT) and Continuous-Time (CT) digital domains. The comparison between the two propositions is highlighted as a trade-off between accuracy and power consumption.

We will first introduce and define the characteristics of ICG signals and the hemodynamic features that can be extracted, including SV. Then, in Section III, the two system architectures in DT and CT digital domains will be described. Finally, Section IV will present the simulation method and the obtained results, followed by their interpretation.

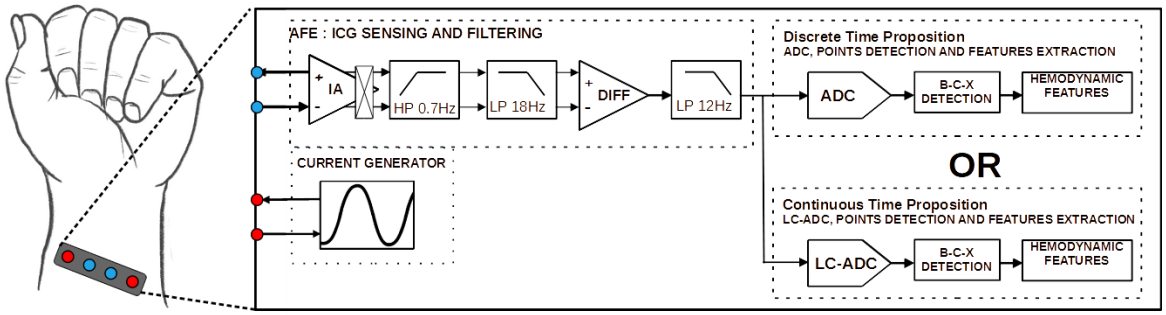

Fig.1. Overview of an ICG system for hemodynamic monitoring with two architecture proposals for B-C-X points detection and features extraction in DT and CT digital domains.

Current work has been supported by CHIST-ERA grant JEDAI, Irish Research Council and French Research Agency project ANR-19-CHR3-0005-01 and EU Regional Development Fund (Estonian Centre of Excellence in ICT Research EXCITE TAR16013 and Mobilitas+ project Mobera20),

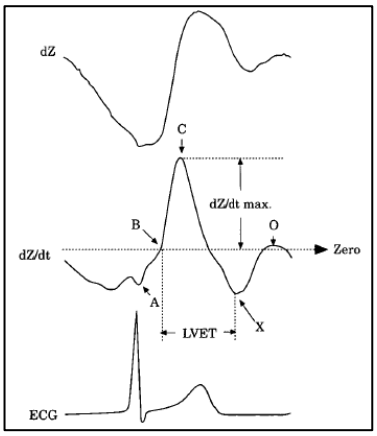

Fig.2. ICG signals dZ, dZ/dT with its characteristic points and a related ECG beat from [1].

II. Stroke Volume, Hemodynamic Features, and ICG Characteristic Points

A. ICG and characteristic points

ICG is a non-invasive method of assessment of heart operation. Typically, it measures the impedance variation on the body caused by changes in blood volume by applying a 20-100 kHz AC current of low intensity between two electrodes, as shown in Fig. 1. The resulting voltage is sensed with another pair of electrodes. ICG is often combined with other measurements such as electrocardiography (ECG) or photoplethysmography (PPG) [11].

The acquired ICG signal Z is not used directly. Most of the ICG applications rely on the derivative dZ/dT, because it is directly linked to the variation of blood volume and contains characteristic points representing different steps of the cardiac activity. There are typically 5 ICG signal characteristics points extracted per heartbeat from dZ/dT [1], as illustrated in Fig. 2.

Point A is related to the contraction of the atria. Point B is associated with the aortic valve opening and can be defined as the dZ/dT zero-crossing before maximum. Point C is the ventricular contraction and defined as $(dZ/dT)_{max}$. Point X relates to the closure of the aortic valve with ventricular contraction and is defined as $(dZ/dT)_{min}$. Finally, point O is the opening of the mitral valve.

B. Stroke Volume definition and Hemodynamic features

The stroke volume is the volume ejected by the heart during each beat and is considered as one of the main hemodynamic parameters. Stroke volume typical values stand between 70 mL and 150 mL. There are numerous definitions of the SV calculation, but the most common formula is the one established by Kubicek [1] [3]. It depends on the B, C, and X points values and timings and a few constants:

$$SV = p\left(\frac{L}{Z_0}\right)^2 . LVET . \left(\frac{dZ}{dT}\right)_{max} \quad (1)$$

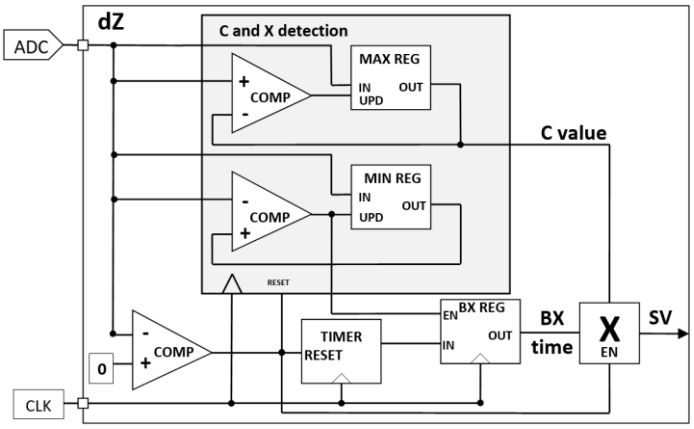

Fig.3. Discrete Time architecture B-C-X and Hemodynamic features detection.

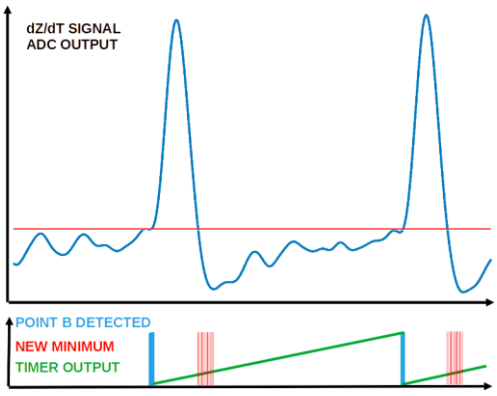

Fig.4. Behavior of the architecture showing the detection of point B, the timer output, and the detection of new minimums to achieve SV calculation.

p is the blood resistivity, assumed constant for SV calculation. The typical value is 135 Ω.cm. L is the length of the conductor (distance between electrodes) and is approximated as 17% of the patient's height. Zo is the mean basal impedance and is typically the transthoracic quasi-static base impedance (20-50 Ω). $LVET$ is the Left Ventricular Ejection Time (time between B and X points). $(dZ/dT)_{max}$ is equal to the point C value. According to Bernstein's data [3], mean values of L, Zo, $LVET$, and $(dZ/dT)_{max}$ are respectively 29.07 cm, 22.7 Ω, 0.26 s, and 0.661 $\Omega.s^{-1}$. By removing the constant components, a simplified SV formula is obtained:

$$SV = LVET . \left(\frac{dZ}{dT}\right)_{max} \quad (2) \; ; \quad SV = (B - X)_{time} . C_{value} \quad (3)$$

SV calculation allows the calculation of derived hemodynamic parameters such as the Cardiac Output (CO) and the Cardiac Index (CI), provided the heart rate is extracted by ECG or ICG and that the body surface area is constant for a given patient. The ICG B, C, and X characteristics points have been manually detected for each record. The corresponding time value, the B-X interval value, the C point amplitude, and the calculated SV are used as our reference data.

$$CO = \frac{SV}{Heart\ Rate}\ ;\ CI = \frac{CO}{Body\ Surface\ Area} \qquad (4)$$

Considering the simplified SV formula (3), our study will focus only on the detection of the ICG B, C, and X characteristic points.

C. Database

The study uses a database acquired by Andrei Krivošei at TalTech, Tallinn, Estonia. This database contains 56 ICG records measured from the wrist and sampled at 200 Hz with a 16-bits resolution, some are annotated with arrhythmia or motion artifacts. The duration of the records varies from 20 seconds to a few minutes. This database is advantageous because the ICG signal is sensed at the wrist, making it easier to envision a wearable wrist-worn system.

III. Architectures for Points Detection and Stroke Volume Extraction

A. ICG measurement system architecture proposal

For ICG impedance signal sensing, a low-intensity 20-100 kHz AC current is generated by a current generator and applied between two electrodes on the body. This current is sensed through another pair of electrodes to measure the impedance Z, as shown in Fig. 1. The Analog Front-End (AFE) amplifies and mixes down the sensed Z signal before filtering. Filtering removes parasitics, motion artifacts, and non-ICG-related frequencies. A differentiator generates the dZ/dT signal. This signal is then converted into the digital domain using either a Nyquist-based ADC in the DT reference architecture or a Level-Crossing ADC (LC-ADC) in the CT reference architecture.

After analog-to-digital conversion, a fully digital system, that is similar in both DT and CT cases, will detect the ICG B, C, and X points and extract hemodynamic features such as SV. The main difference between the DT and CT digital architectures lies in the presence of a clock in the DT case, while the CT case is an event-driven version of the digital computations. This study will focus on the digital part of the ICG system, to prove that a simple and low-power digital implementation can achieve a sufficient SV measurement accuracy leading to the opportunity of a SoC design. Also, we want to determine if event-driven CT is advantageous or not in the case of ICG. This is motivated by the fact that this signal processing scheme is very beneficial for processing signals that are sparse in time, such as ECG signals [12].

B. Discrete-Time Architecture

This part describes the B-C-X detection and Hemodynamic Features blocks in Fig. 2. The system of Fig. 3 takes as input the ADC output data to detect the ICG B-C-X characteristic points and to process the LVET time and C value to achieve SV calculation.

Considering that we focus on the estimation of SV, and according to Equation (3), the system needs to detect and measure the E amplitude value and the time interval between points B and X, also named LVET time.

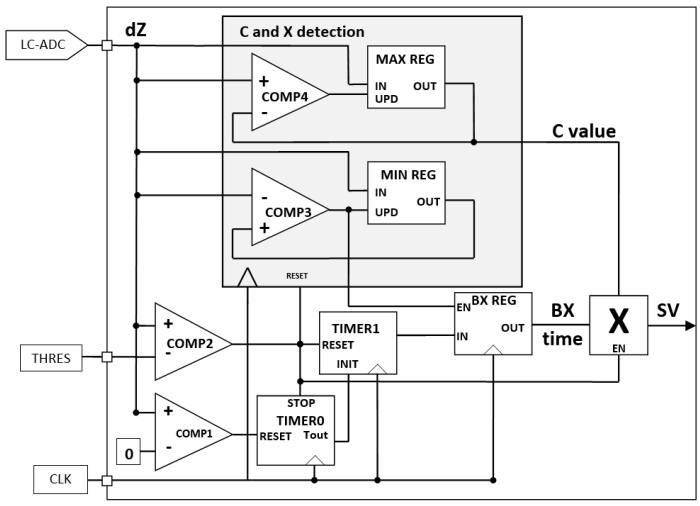

Fig.5. Improvement of the architecture of Fig. 3, to consider non-ideal signal shapes.

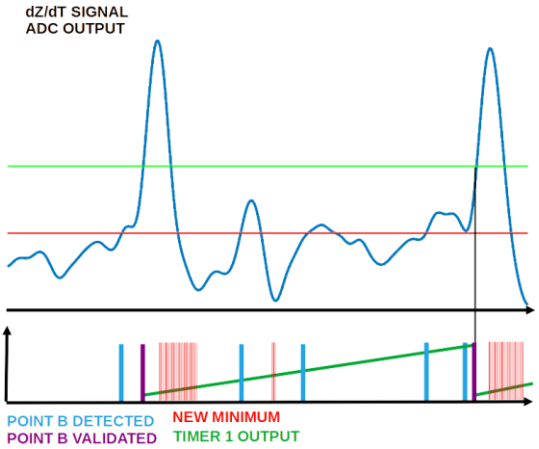

Fig.6. Behavior of the architecture showing the detection of point B, the timer output, the zero and upper thresholds and the detection of new minimums to achieve SV calculation.

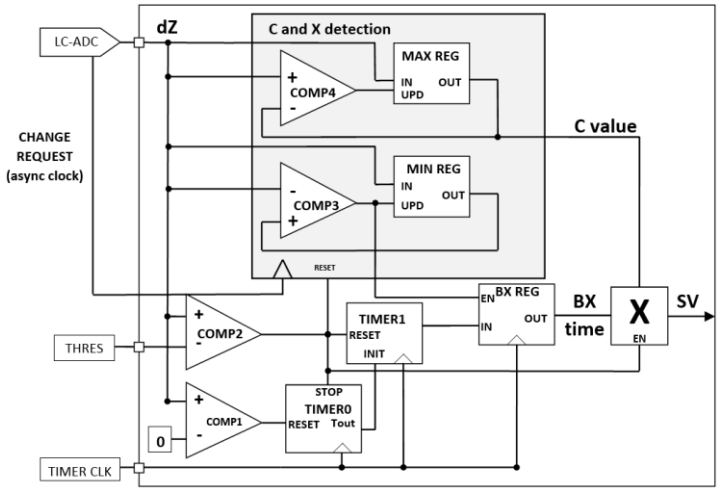

Fig.7. Continuous Time architecture of blocks B-E-X detection and Hemodynamic features from Fig. 2.

Fig. 3 shows the block-level schematic and Fig. 4 details its behavior. The B point is detected using a rising-edge zero-crossing detector that activates the detection of E and X points and starts a timer. Point E is detected as the maximum. Each new dZ/dT sample is compared to the previous sample to verify if it is a new maximum or not. If the condition is satisfied, then the value of point E is stored in a dedicated register. The detection of the X point is similar but defined as a minimum detection. When the X point is detected, the timer output is stored and represents the actual B-X time interval. When a new B point is detected, the SV value is calculated as the multiplication of the B-X time by the point E value and the system is reset.

Since ICG signal waveforms are not always consistent and vary largely between individuals, there are particular signal shapes that corrupt the calculated SV value. For instance, there can be multiple zero-crossing points happening between two annotated B points and being detected as a new B point. Also, the minimum value of dZ/dT (X point) is not necessarily the first minimum inflexion point after E point and can be preceded by a local maximum.

To work with real ICG data, the proposed architecture of Fig. 3 is modified, as shown in Fig. 5, to include additional circuitry to deal with the mentioned particularities. Its behavior is described in Fig. 6 and summarized here. In a first step 1, the B point is detected as a rising-edge zero-crossing and Timer 0 is started. Next, the detected B point is considered correct if the signal crosses an upper-level threshold, Timer 0 stops and Timer 1 starts with an initial loaded value corresponding to the output of Timer 0. This process avoids the detection of false B points, as it can be seen in example of Fig. 6. The third step consists of detecting E and X points, respectively as maximum and minimum, like in Fig 3. When a new minimum is detected, the output value of Timer 1 is stored in a dedicated register. Finally, when a new B point is validated, the SV value is computed, and the system is reset.

C. Event-driven Continuous Time Architecture

To quantify the benefits of the event-driven continuous-time digital architecture, Table I shows the number of generated samples using an LC-ADC applied on an oversampled ICG signal. The power consumption of the feature extraction circuits is proportional to the number of samples. This Table shows that a 7-bit LC-ADC generates an equivalent number of samples compared to a 200 Hz DT processing, while a 5-bit LC-ADC corresponds to an 80 Hz DT system. In addition, study of the power-efficiency of LC-ADC on biosignals such as ECG [12] highlights that for low resolution (<8-bit) applications, an LC-ADC is more power-efficient than a SAR-ADC. Thus, an event-driven CT system could decrease consumption at system-level (decreased consumption for the ADC) as well as a reduction of the number of operations because the number of samples is reduced. These two considerations should be beneficial for ICG-based integrated feature extraction.

Fig. 7 presents the architecture of the event-driven CT system. It is very similar to the DT architecture, except that the output of the LC-ADC is now asynchronous and that the E and X detection registers are using the changes in the LC-ADC output as an asynchronous clock. The measurement of SV is dependent on B-X time interval. For simplicity and comparison, clocked timers are still used for this purpose, thus the detailed system is partly asynchronous (clockless) and partly clocked for the timers. It is to note that clockless time measurement schemes can replace the traditional clocked timers to realize a totally clockless architecture [13].

IV. Simulation and Results

After the text edit has been completed, the paper is ready for the template. Duplicate the template file by using the Save As command, and use the naming convention prescribed by your conference for the name of your paper. In this newly created file, highlight all of the contents and import your prepared text file. You are now ready to style your paper; use the scroll down window on the left of the MS Word Formatting toolbar.

A. SV accuracy and comparison parameters

The Discrete Time and Continuous Time architecture presented in the previous section have been modelled in Matlab Simulink. The simulations have been done on 13 records, one of them marked with arrhythmia, for a total of 312 heartbeats.

Stroke Volume is computed on both architectures, associated with the corresponding median and standard deviation. The measured Stroke Volume is normalized to its reference value:

$$SV_{normalized} = \frac{SV_{measured}}{SV_{reference}}$$

The median represents the value where the measurement values tend to be centered, knowing that the difference between the reference and the median can be compensated by system calibration. The standard deviation is thus the main parameter for the system measurement accuracy. It shows the measurement deviation from the reference and thus the error probability. The results are shown in Table II.

B. Discrete Time Results Interpretation

The results from Table II show different trends for the Discrete Time architecture:

TABLE I. NUMBER OF ICG SAMPLES GENERATED BY LC-ADC

LC-ADC bits	**7**	**6**	**5**
Generated samples/min	11 184	7206	4894
Equivalent sampling frequency	200 Hz	120 Hz	80 Hz

TABLE II. NORMALIZED STROKE VOLUME SIMULATION RESULTS

	DT 200 Hz		**DT 120 Hz**		**DT 80 Hz**		**CT**	
	median	***std***	***median***	***std***	***median***	***std***	***median***	***std***
16-bits	0.9904	0.0909	0.9817	0.0919	0.9680	0.1248	-	-
8-bits	0.9756	0.0998	0.9727	0.1018	0.9602	0.1156	0.9789	0.1018
7-bits	0.9642	0.1053	0.9616	0.1053	0.9542	0.1061	0.9681	0.1133
6-bits	0.9463	0.1026	0.9436	0.1020	0.9381	0.1075	0.9482	0.1166
5-bits	0.9138	0.1167	0.9116	0.1161	0.9054	0.1194	0.9199	0.1879

- The precision decreases with the frequency for resolutions superior to 8 bits.
- For resolutions lower than 7 bits (6-5 bits), decreasing the frequency does not affect the precision. This is due to the fact that the quantification impact is higher than sampling error.
- Reducing the number of bits tends to have lower median SV value, because the C point error values itself tends to be reduced proportionally to the quantification error.
- The standard deviation varies from 9% to 13%.

The results obtained in Discrete Time show that it is possible to obtain SV measurement with an error inferior to 13%. using a simple system with a reduced resolution and sampling frequency. The measurement results for Discrete Time are detailed in TABLE III.

B point timing error depends only on the sampling frequency. Its median value is equal to half the sampling period. Timing error is positive because the detection method for B point makes that it cannot be detected in advance. C point measured amplitude is reduced by an error of 1 LSB. We can also observe that the error increases when we decrease the sampling frequency whereas at 5bits the sampling frequency has no more effect. The median value of the normalized measured Stroke Volume is closer to the reference when sampling frequency is lower. Practically it is undermined by an increased standard deviation.

C. Continuous Time Results Interpretation

The results from Table II shows different trends for the Continuous Time architecture. For a limited resolution (6-5 bits) the median value of measured SV tends to be lower than the SV reference. This is because both the C point and the BX time interval measured value tends to be lowered. The C point value is smaller because of the quantification error. The BX time interval is shorter because point X tends to be detected before it really happens due to the resolution and the way point X is detected. The measurement results are detailed in Table IV. Standard Deviation is 11.66% at 6bits and 18.79% at 5bits.

D. Discrete Time and Continuous Time Comparison

After compensating the normalized SV deviation by the median (Table V), values that are presented in Fig.9, we can observe that there is no configuration in which Continuous Time is superior. In fact, the results show that even for an equivalent complexity or power consumption the deviation obtained with the CT architecture is higher. For instance, even for low-frequency 80Hz sampling, it appears that DT configuration is more accurate than CT at an equivalent complexity (13.19% deviation against 20.43%). From this observation, we can conclude that CT is not suited for SV measurement.

E. Acceptable values for Stroke Volume measurement error

In the previous stage we have interpreted the results in function of the architecture configuration and compared the efficiency of these configurations. The question now to address is to determine if the SV measurement accuracy is sufficient for practical use. One method for this purpose is the Bland-Altman analysis [14]. Commonly used for determination of medical measurement methods [11], [15], this analysis allow to compare two measurement methods, one of them considered as the reference method, by the assessment of the agreement between these two methods. One common criteria for cardiac output (CO=SVxHR) measurement solutions is that a new measurement method is considered as not sufficiently accurate if 30% of the measurements are outside the limits of agreement [17].

TABLE III. DT DETAILED SIMULATION RESULTS

Resolution	Sampling Frequency (Hz)	B median timing error (ms)	X median timing error (ms)	BX median timing error (ms)	C amplitude error median value (LSB)	SV normalized median value
16bits	200	1.7	-0.4	-2.9	-	0.9904
16bits	120	4	0	-4.2	-	0.9817
16bits	80	6.2	0	-7.1	-	0.9680
6bits	200	1.7	-8.3	-9.6	-0.57	0.9463
6bits	120	4	-6.3	-9.6	-0.65	0.9436
6bits	80	6.2	-5.2	-11.11	-0.76	0.9381
5bits	200	1.7	-12.5	-15	-0.51	0.9138

TABLE IV. CT DETAILED SIMULATION RESULTS

Resolution	B median timing error (ms)	X median timing error (ms)	BX median timing error (ms)	C amplitude error median value (LSB)	SV normalized median value
CT 6bits	-0.6	-10.6	-9.6	-0.53	0.9484
CT 5bits	-0.5	-14.6	-12.7	-0.47	0.9202

TABLE V. NORMALIZED STROKE VOLUME SIMULATION RESULTS AFTER MEDIAN COMPENSATION

	DT 200 Hz		DT 120 Hz		DT 80 Hz		CT	
	median	*std*	*median*	*std*	*median*	*std*	*median*	*std*
16bits	1	0.0918	1	0.0936	1	0.1289	-	-
8-bits	1	0.1023	1	0.1047	1	0.1204	1	0.1040
7-bits	1	0.1092	1	0.1095	1	0.1112	1	0.1170
6-bits	1	0.1084	1	0.1081	1	0.1146	1	0.1230
5-bits	1	0.1277	1	0.1274	1	0.1319	1	0.2043

TABLE VI. BLAND-ALTMAN ANALYSIS RESULTS (% OF SV MEASUREMENTS OUTSIDE THE LIMITS OF AGREEMENT)

	16-bits	7-bits	6-bits	5-bits
200Hz	reference	14	18	25
120Hz	5.7	15	18	25
80Hz	12	14	19	27
CT	-	17	20	32

In our particular case we use the results obtained with the 16bits-200Hz configuration as our reference measurement method because we consider that these results are the best that can be obtained giving the 200Hz sampling rate of the original data. After applying the Bland-Altman method to the other configuration results, we obtain the results of Table VI. One example of the Bland-Altman plot obtained with the simulated results is shown in Fig. 8 we observe that for all the DT configuration there is always less than 30% of the measurements outside the limits of agreement.

V. Conclusion

This paper discussed the opportunity of a simple wearable system for ICG Stroke Volume measurement for heart state monitoring purposes and the interest raised by Continuous Time data alternative. Results revealed that even for low configuration and a reduced sampling frequency, the Discrete Time flavor system error varies from 9% to 13% and can be considered as sufficient for leisure or commercial activities as the Bland-Altman analysis revealed at worst 27% of the measurements outside the limit of agreement. The second answer from this work is that Continuous Time alternative, that was supposed to be more efficient, is actually less precise than Discrete Time for a same system complexity and power-consumption, thus Continuous Time data is not advantageous. The results lead also to the feasibility of the use of ICG in simple systems dedicated to heart state low-power monitoring, combined or not with other biosignals such as ECG.

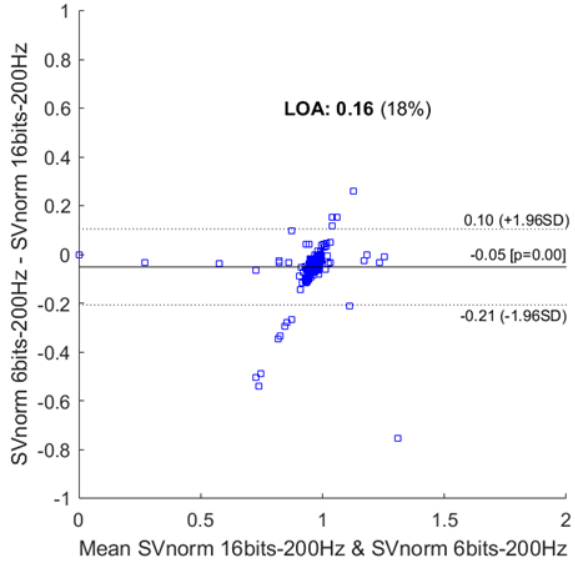

Fig.8. Bland-Altman plot of results obtained with the 6bits-200Hz configuration.

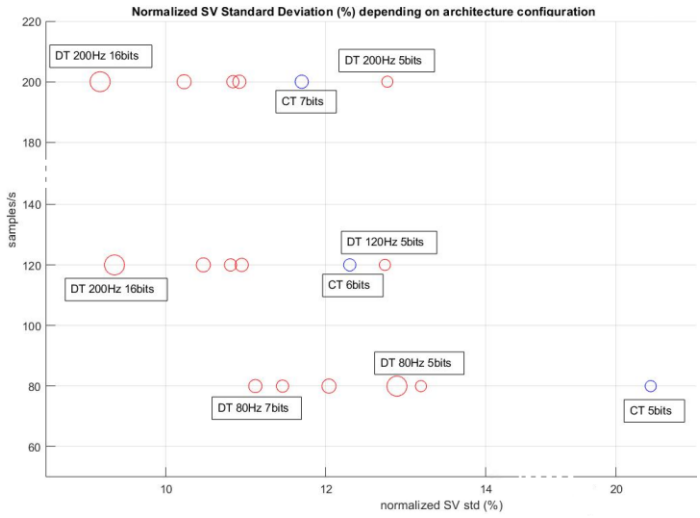

Fig.9. Comparison graph of the different architecture configurations

References

[1] H. H. Woltjer, H. J. Bogaard, and P. M. J. M. De Vries, "The technique of impedance cardiography," *Eur. Heart J.*, vol. 18, no. 9, pp. 1396–1403, 1997, doi: 10.1093/oxfordjournals.eurheartj.a015464.

[2] R. P. Patterson, "Fundamentals of Impedance Cardiography," *IEEE Eng. Med. Biol. Mag.*, vol. 8, no. 1, pp. 35–38, 1989, doi: 10.1109/51.32403.

[3] D. P. Bernstein and H. J. M. Lemmens, "Stroke volume equation for impedance cardiography," *Med. Biol. Eng. Comput.*, vol. 43, no. 4, pp. 443–450, 2005, doi: 10.1007/BF02344724.

[4] J. Bour and J. Kellett, "Impedance cardiography - A rapid and cost-effective screening tool for cardiac disease," *Eur. J. Intern. Med.*, vol. 19, no. 6, pp. 399–405, 2008, doi: 10.1016/j.ejim.2007.07.007.

[5] X. Chen *et al.*, "Noninvasive ambulatory monitoring of the electric and mechanical function of heart with a multifunction wearable sensor," *Proc. - IEEE 38th Annu. Int. Comput. Softw. Appl. Conf. Work. COMPSACW 2014*, pp. 662–667, 2014, doi: 10.1109/COMPSACW.2014.111.

[6] T. Ahrens, "The most important vital signs are not being measured," *Aust. Crit. Care*, vol. 21, no. 1, pp. 3–5, 2008, doi: 10.1016/j.aucc.2007.12.061.

[7] C. J. Kirkpatrick, "Exploring Exciting Frontiers in Europe," *IEEE Eng. Med. Biol. Mag.*, no. June, pp. 53–59, 2007.

[8] A. Hafid, S. Benouar, M. Kedir-Talha, F. Abtahi, M. Attari, and F. Seoane, "Full Impedance Cardiography Measurement Device Using Raspberry PI3 and System-on-Chip Biomedical Instrumentation Solutions," *IEEE J. Biomed. Heal. Informatics*, vol. 22, no. 6, pp. 1883–1894, 2018, doi: 10.1109/JBHI.2017.2783949.

[9] D. Sopic, S. Murali, F. Rincón, and D. Atienza, "Touch-based system for beat-to-beat impedance cardiogram acquisition and hemodynamic parameters estimation," *Proc. 2016 Des. Autom. Test Eur. Conf. Exhib. DATE 2016*, pp. 726–731, 2016, doi: 10.3850/9783981537079_0702.

[10] H. Yazdanian, A. Mahnam, M. Edrisi, and M. Esfahani, "Design and implementation of a portable impedance cardiography system for noninvasive stroke volume monitoring," *J. Med. Signals Sens.*, vol. 6, no. 1, pp. 47–56, 2016, doi: 10.4103/2228-7477.175871.

[11] J. Sola *et al.*, "Noninvasive and nonocclusive blood pressure estimation via a chest sensor," *IEEE Trans. Biomed. Eng.*, vol. 60, no. 12, pp. 3505–3513, 2013, doi: 10.1109/TBME.2013.2272699.

[12] J. Van Assche and G. Gielen, "Power Efficiency Comparison of Event-Driven and Fixed-Rate Signal Conversion and Compression for Biomedical Applications," *IEEE Trans. Biomed. Circuits Syst.*, vol. 14, no. 4, pp. 746–756, 2020, doi: 10.1109/TBCAS.2020.3009027.

[13] Z. Wang *et al.*, "Chip for AIoT Devices Using Asynchronous Spike-Based Feature Extractor and Convolutional Neural Network," vol. 16, pp. 200–202, 2021.

[14] P. P. Wang, C. Zhang, H. Yang, D. Bharadia, and P. P. Mercier, "ISSCC 2020 SESSION 20 Low-Power Circuits for IoT & Health," *2020 IEEE Int. Solid- State Circuits Conf. -*, pp. 314–316, 2020.

[15] D. Giavarina, "Understanding Bland Altman analysis," *Biochem. Medica*, vol. 25, no. 2, pp. 141–151, 2015, doi: 10.11613/BM.2015.015.

[16] P. M. Odor, S. Bampoe, and M. Cecconi, "Cardiac Output Monitoring: Validation Studies–how Results Should be Presented," *Curr. Anesthesiol. Rep.*, vol. 7, no. 4, pp. 410–415, 2017, doi: 10.1007/s40140-017-0239-0.